An Energy-Efficient IEEE 802.11ad Mesh Network for Seismic Acquisition

Varun Amar Reddy, Gordon L. Stüber
Center for Energy and Geo Processing
School of Electrical & Computer Engineering
Georgia Institute of Technology
Atlanta, GA 30332, USA
varun.reddy@gatech.edu, stuber@ece.gatech.edu

Suhail Al-Dharrab, Ali Hussein Muqaibel, Wessam Mesbah
Center for Energy and Geo Processing
Electrical Engineering Department
King Fahd University of Petroleum & Minerals
Dhahran 31261, Saudi Arabia
{suhaild, muqaibel, mesbahw}@kfupm.edu.sa

***Abstract*—Modern seismic surveys can obtain subsurface images of superior quality and depth, albeit requiring wireless acquisition systems to keep up with higher data rate requirements. Data communication protocols have been studied primarily for links between the geophones and the gateway nodes, leaving a dearth of analysis for the communication links between the gateway nodes and the sink node. In this paper, a novel wireless geophone network architecture based on the IEEE 802.11ad standard is proposed with the objective of providing gigabit rates in order to support real-time seismic acquisition. A performance analysis reveals that the latency and power consumption are dependent on the ratio of the data generation rate to the data transfer rate. An additional Power-Saving Geophone Relay (PSGR) scheme is described, which exploits idle periods of operation to conserve power at the cost of an increased latency. The trade-off between the latency and power consumption under the PSGR scheme is evaluated for a variety of scenarios in seismic acquisition.**

I. Introduction

Seismic surveys are carried out over areas as large as 100 km^2 to scout for oil and gas reserves by generating subsurface images of the Earth [1]. Vibroseis trucks periodically move around the survey area and generate seismic waves, termed as a *sweep*, that travel into the ground, get reflected by subsurface layers, and are subsequently recorded by a large number of devices called *geophones*. The data is aggregated at the *Data Collection Center (DCC)* for subsequent processing.

Real-time seismic data acquisition at the DCC is of vital importance, which would allow the field engineers to adaptively modify the nature of subsequent sweeps based on the data obtained from the current sweep. Considering the use of 14,400 geophones, each generating data at a rate of 144 kbps, an effective rate of around 2 Gbps is perceived at the DCC.

Although cable can serve as a rapid and reliable mode of data transfer, it accounts for a majority of the equipment weight, maintenance and labor costs of seismic surveys, and also exerts an adverse impact on the ecosystem [2]. Hence, there has been a strong interest in developing wireless architectures and power conservation schemes for seismic acquisition (Ultra-wideband [3], IEEE 802.11n/ac [4], IEEE 802.11af [5], [6], IEEE 802.11ad with self organizing ad hoc network [7]), but only at the lowest layer of the architecture, i.e. for direct communication links with the geophones. In [8], the latency performance at the topmost layer (at the DCC) has been evaluated for several types of communication technologies. However, power conservation aspects have not been considered in [8]. A duty-cycling medium access control (MAC) for linear sensor networks has been studied in [9] as a function of the sleep duration and data generation rate. A hybrid CSMA-TDMA approach is proposed in [10] wherein the sleep periods are dynamically alloted based on event occurrence. In [11], a duty-cycled approach is modified to allow selective awakening based on the traffic load conditions.

The contribution of this work is twofold. Firstly, a novel analysis method for estimating the latency and the power consumption in an IEEE 802.11-based mesh network with a large number of hops is discussed. The use of the Transmission Control Protocol (TCP) over 802.11 is also considered. Secondly, an energy-efficient data transfer scheme that is compliant with the IEEE 802.11ad standard is proposed for seismic acquisition. Contrary to prior works [9]–[11], the gigabit-rate requirements imposed by seismic acquisition are taken into account, and the deterministic nature of the traffic and static topology of geophone networks are exploited to save power at the cost of an increased latency.

II. Proposed Network Architecture

A typical seismic survey can deploy up to 14,400 geophones in a grid topology with 30 parallel rows, each comprising 480 geophones [6]. Following the approach in [8], the seismic data from the geophones is first acquired by gateway nodes and subsequently relayed towards the row of geophones at the center of the survey area. A multi-channel dual-radio IEEE 802.11ad mesh network is proposed for use at this stage, as shown in Fig. 1a, wherein the geophones themselves take part in the final relaying process towards the DCC. The IEEE 802.11ad standard [12] is an ideal choice, given its ability to sustain real-time seismic acquisition by achieving data rates of up to 6.7 Gbps over unlicensed channels in the 60 GHz bands. Each geophone can be equipped with two radios that operate on unique channels. The geophones are

This work is supported by the Center for Energy and Geo Processing at Georgia Institute of Technology and King Fahd University of Petroleum and Minerals, under grant number GTEC1601.

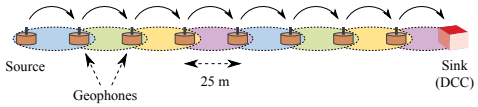

(a) Proposed Network Architecture.

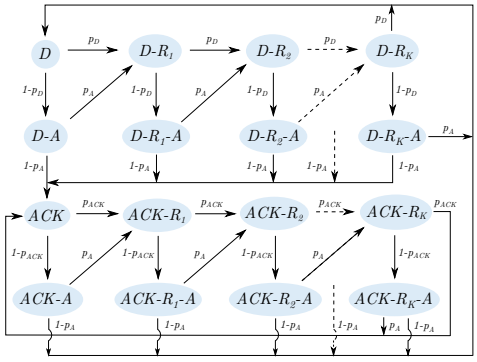

(b) Markov Model for TCP Data Transfer over the IEEE 802.11 EDCA

Fig. 1: System Model

spaced 25 m apart as per seismic acquisition requirements, and suitable antenna heights can be employed so as to minimize the amount of co-channel interference among neighboring cells. This implies that concurrent transmissions can occur between all the pairwise geophones at any point of time, thereby enabling high-rate data transfer towards the DCC. Single-hop static routing can be applied since the entire geophone network topology is fixed for long durations of time.

Given that h denotes the geophone antenna height and d denotes the distance between adjacent geophones, the total path loss $L_{\text{FE}}(h,d)$ is computed after taking into account the impact of ground reflection and the atmospheric absorption loss in the 60 GHz bands [7].

$$L_{\text{FE}}(h,d) = \left(\frac{c}{4\pi f d}\right)^2 \left|1+\Gamma_{\perp} e^{j4\pi f h^2/cd}\right|^2 \times 1.003922^{-d} \quad (1)$$

where $f = 60$ GHz and $\Gamma_{\perp}$ is the reflection coefficient. The beamforming process given in the 802.11ad standard would have to be performed just between adjacent geophones, and only at the start of the seismic survey process since the geophones remain at fixed positions. In order to operate at a raw data rate of 6.237 Gbps, the minimum receiver sensitivity is -49 dBm [12]. For a transmit power $P_t = 10$ dBm, a realized antenna gain $G = 17$ dB, and $h = 0.2$ m, a straightforward computation of the received power P_r reveals that such a link is feasible.

$$P_r = P_t G^2 L_{\text{FE}}(0.2, 25) \approx -46 \text{ dBm} \quad (2)$$

The default channel access scheme is provided by *Enhanced Distributed Channel Access* (EDCA) [12], which is based on carrier sense multiple access with collision avoidance (CSMA/CA) and binary exponential backoff. For each transmission, a backoff time slot value is introduced that is drawn uniformly from the interval $[0, CW]$, $CW \in [CW_{\text{min}}, CW_{\text{max}}]$. The value of CW is doubled up to a maximum of K retransmissions (when it attains the value of CW_{max}) and is reset back to CW_{min} upon a successful transmission.

TABLE I: Definition of Time-Specific Parameters

Notation	Description
SIFS	Short Interframe Space
AIFS	Arbitration Interframe Space
t_{slot}	Slot Time
t_h	Transmission time of header of a data frame
t_a	Transmission time of an 802.11ad acknowledgment frame
t_d	Transmission time of payload of a data frame (TCP Data)
t_{ack}	Transmission time of payload of a data frame (TCP ACK)

As shown in Fig. 1b, a semi-Markov process [13] is used to represent the transmission of a TCP data segment (denoted by D) and up to K retransmissions (denoted by $D-R_k$, $1 \le k \le K$) along with the subsequent 802.11 acknowledgments (denoted by $D-A$ and $D-R_k-A$). This is followed by the TCP acknowledgment (denoted by ACK) and its associated retransmissions and acknowledgments. The packet error probability p_S is a function of the packet size corresponding to state S, attenuation effects introduced by the channel, and the receiver noise. Assuming no TCP timeouts and delayed TCP acknowledgments, the nature of p_S is determined by the perceived SINR alone since there are no collisions that are introduced as a result of the EDCA. Let the state S be associated with a certain duration of time T_S.

$$\begin{aligned}
T_D &= AIFS + (CW_{\text{min}} - 1)\cdot t_{slot}/2 + t_h + t_d \\
T_{D-R_k} &= AIFS + (2^k \cdot CW_{\text{min}} - 1)\cdot t_{slot}/2 + t_h + t_d \\
T_{ACK} &= AIFS + (CW_{\text{min}} - 1)\cdot t_{slot}/2 + t_h + t_{ack} \\
T_{ACK-R_k} &= AIFS + (2^k \cdot CW_{\text{min}} - 1)\cdot t_{slot}/2 + t_h + t_{ack} \\
T_{D-A} &= T_{ACK-A} = T_{D-R_k-A} = T_{ACK-R_k-A} \\
&= SIFS + t_a
\end{aligned}$$

The various notations are specified in Table I. Let the steady state probability of state S be denoted by ϕ_S. For a standards-compliant value of $K = 6$, the values for ϕ_S are obtained in (3)-(5). The values for ϕ_S pertaining to the TCP ACK can be obtained by swapping the subscript D with ACK in (3)-(5).

$$\phi_D = \frac{1 - p_{ACK}}{(4 - 3p_{ACK} - 3p_D + 2p_{ACK}\,p_P)\sum_{k=0}^{K}(p_D + p_A - p_D\,p_A)^k} \quad (3)$$

$$\phi_{D-R_k} = \phi_D \cdot (p_A + p_D - p_A p_D)^k \quad (4)$$

$$\phi_{D-A} = \phi_D \cdot (1 - p_D) \quad (4)$$

$$\phi_{D-R_k-A} = \phi_D \cdot (1-p_D)\cdot (p_A + p_D - p_A p_D)^k \quad (5)$$

Let π_S denote the proportion of time that the semi-Markov process spends in state S. The value of π_S can be expressed as the weighted average of the steady-state probabilities, where the weights are given by the duration spent in each state [13]. For the states $S_D = \{D, D-R_k, D-A, D-R_k-A\}$ pertaining to the TCP data segment, an expression for $\pi_s, s \in S_D$ is given in (6).

$$\pi_s = \frac{\phi_s \cdot T_s}{\sum_{s' \in S_D} \phi_{s'} \cdot T_{s'}} \quad (6)$$

Similar expressions for the states pertaining to the TCP ACK can be obtained by swapping the subscript D with ACK. A

formulation can now be made for τ, which denotes the time required for a single TCP Data-ACK exchange, by accounting for those instances where the TCP data segment or ACK would have to be resent after K retransmissions at the MAC layer.

$$\tau = \left(\frac{\pi_D}{T_D} - \frac{\pi_{D-R_K}}{T_{D-R_K}} - \frac{\pi_{D-R_K-A}}{T_{D-R_K-A}}\right)^{-1} + \left(\frac{\pi_{ACK}}{T_{ACK}} - \frac{\pi_{ACK-R_K}}{T_{ACK-R_K}} - \frac{\pi_{ACK-R_K-A}}{T_{ACK-R_K-A}}\right)^{-1} \quad (7)$$

Two additional parameters are introduced: R_b, which denotes the buffering or data generation rate at the source geophone, and R_d, which represents the data transfer rate between adjacent geophones. An expression for the total time required, say $\mathcal{T}$, for the transfer of α packets, each of size P, across N geophones can be formulated accordingly.

$$\mathcal{T} = \begin{cases} \frac{\alpha P}{R_b} + (N-1)\cdot\tau & , \quad R_b < R_d \\ (\alpha + N - 2)\cdot\tau & , \quad R_b \geq R_d \end{cases} \quad (8)$$

When $R_b < R_d$, $\mathcal{T}$ is limited by the value of R_b that is introduced as a buffering delay, in addition to a finite relaying delay that is a function of the number of hops and τ. For the case when $R_b \geq R_d$, the overall latency is limited by the value of τ alone, since there is no buffering delay. An expression for the latency $\mathcal{L}$ can be obtained from (8) as $\mathcal{T} - (\alpha P/R_b)$.

The analysis can be extended to the computation of the average power consumption as well. The state S is associated with an amount of energy $E_{S,tx}$ or $E_{S,rx}$ depending on whether a geophone is transmitting or receiving respectively.

$$\begin{aligned} E_{D,tx/rx} &= (AIFS + (CW_{\min} - 1)\cdot t_{slot}/2)\cdot I_{idle}\cdot V + (t_h + t_d)\cdot I_{tx/rx}\cdot V \\ E_{D-R_k,tx/rx} &= \left(AIFS + (2^k CW_{\min} - 1)\cdot t_{slot}/2\right)\cdot I_{idle}\cdot V + (t_h + t_d)\cdot I_{tx/rx}\cdot V \\ E_{ACK,tx/rx} &= (AIFS + (CW_{\min} - 1)\cdot t_{slot}/2)\cdot I_{idle}\cdot V + (t_h + t_{ack})\cdot I_{tx/rx}\cdot V \\ E_{ACK-R_k,tx/rx} &= \left(AIFS + (2^k CW_{\min} - 1)\cdot t_{slot}/2\right)\cdot I_{idle}\cdot V + (t_h + t_{ack})\cdot I_{tx/rx}\cdot V \\ E_{D-A,tx/rx} &= E_{ACK-A,tx/rx} = E_{D-R_k-A,tx/rx} \\ &= E_{ACK-R_k-A,tx/rx} \\ &= SIFS\cdot I_{idle}\cdot V + t_a\cdot I_{tx/rx}\cdot V \end{aligned}$$

where I_{tx}, I_{rx}, I_{idle} denote the value of the current in transmit, receive, idle modes respectively and V is the supply voltage. For a given geophone, the total energy consumption associated with the transmission (E_{tx}) and reception (E_{rx}) of α packets can be computed using (10) and (11) respectively. The average power consumption per geophone P_{avg} can now be found by summing up the contributions for all N geophones.

$$P_{\text{avg}} = \frac{(N-1)\cdot[E_{tx} + E_{rx} + 2\cdot(\mathcal{T} - \alpha\tau)\cdot I_{idle}\cdot V]}{N\cdot\mathcal{T}} \quad (9)$$

III. Power-Saving Geophone Relay (PSGR) Scheme

The PSGR scheme is proposed for reducing power consumption by imposing periods of operation in sleep mode. Its primary features and operation are elucidated below.

A. Key Features

1) Effective Power Conservation: As compared to approaches based on transmit power control, effective power-saving can be achieved by enforcing the geophone to operate in sleep mode [14], wherein the transceiver is switched off to eliminate idle listening and packet overhearing.

2) Uniform Power Consumption: By imposing equivalent sleep periods across all the geophones, uniformity in power consumption can be attained.

3) TCP over Mesh Networks with Large Hop-Count: It is known that TCP is not well-suited for mesh networks with a large number of hops, since an acknowledgment from the receiver that is delayed extensively would be interpreted as packet loss by the transmitter. This problem can be circumvented by maintaining single-hop TCP links between each pair of adjacent geophones, rather than having a dedicated link between each of the geophones and the DCC.

4) Standards-Compliance: The functionality of the proposed scheme can be implemented at the transport and application layers, thereby eliminating the need for any proprietary or licensed hardware.

B. Operation

1) All geophones operate in sleep mode as per a preset duty cycle, such that they awaken at intervals of t_{sleep} to receive impending transmissions. This interval could also be made to coincide with the beacon interval. Given that a node requires at most 250 μs to shift from sleep to idle mode of operation [6], t_{sleep} must be chosen to be larger than this value. This approach would require only pairwise synchronization between adjacent geophones.
2) After $\beta \leq \alpha$ packets have been buffered at the source geophone, say G_a, packet transmission via TCP begins towards the next geophone in line, say G_b. In order to promote further power-saving, G_a can operate in sleep mode for an additional duration of t_{hold}, after which the transmission is begun at the subsequent wake-up instance. G_a and G_b return to operating as per the original sleep cycle upon the completion of the transfer of β packets.
3) In the event that all α packets have been relayed by a geophone, it may operate in sleep mode for longer durations without having to wake-up at intervals of t_{sleep} since there are no more impending transmissions.
4) Steps (2)-(3) are repeated until α data packets have been delivered to the endmost geophone (or the DCC).

IV. Performance Evaluation

The simulation parameters are listed in Table II. In Fig. 2, a comparison between the analysis and simulation results (using ns-3) is shown for three possible scenarios in seismic acquisition, with thicker lines being used to denote the analysis results. Naturally, the latency grows with an increase in both N and α, as can be inferred from (8). When $R_b < R_d$, the latency remains constant since the packets arrive at the DCC after a fixed relaying delay. However, when $R_b > R_d$, the relaying delay is exacerbated for larger values of N and α,

$$E_{tx} = \left(\frac{\alpha\,\tau\,\pi_D}{T_D}\right)E_{D,tx} + \left(\frac{\alpha\,\tau\,\pi_{D-A}}{T_{D-A}}\right)E_{D-A,rx} + \sum_{k=1}^{K}\left[\left(\frac{\alpha\,\tau\,\pi_{D-R_k}}{T_{D-R_k}}\right)E_{D-R_k,tx} + \left(\frac{\alpha\,\tau\,\pi_{D-R_k-A}}{T_{D-R_k-A}}\right)E_{D-R_k-A,rx}\right] + \left(\frac{\alpha\,\tau\,\pi_{ACK}}{T_{ACK}}\right)$$
$$E_{ACK,rx} + \left(\frac{\alpha\,\tau\,\pi_{ACK-A}}{T_{ACK-A}}\right)E_{ACK-A,tx} + \sum_{k=1}^{K}\left[\left(\frac{\alpha\,\tau\,\pi_{ACK-R_k}}{T_{ACK-R_k}}\right)E_{ACK-R_k,rx} + \left(\frac{\alpha\,\tau\,\pi_{ACK-R_k-A}}{T_{ACK-R_k-A}}\right)E_{ACK-R_k-A,tx}\right] \quad (10)$$

$$E_{rx} = \left(\frac{\alpha\,\tau\,\pi_D}{T_D}\right)E_{D,rx} + \left(\frac{\alpha\,\tau\,\pi_{D-A}}{T_{D-A}}\right)E_{D-A,tx} + \sum_{k=1}^{K}\left[\left(\frac{\alpha\,\tau\,\pi_{D-R_k}}{T_{D-R_k}}\right)E_{D-R_k,rx} + \left(\frac{\alpha\,\tau\,\pi_{D-R_k-A}}{T_{D-R_k-A}}\right)E_{D-R_k-A,tx}\right] + \left(\frac{\alpha\,\tau\,\pi_{ACK}}{T_{ACK}}\right)$$
$$E_{ACK,tx} + \left(\frac{\alpha\,\tau\,\pi_{ACK-A}}{T_{ACK-A}}\right)E_{ACK-A,rx} + \sum_{k=1}^{K}\left[\left(\frac{\alpha\,\tau\,\pi_{ACK-R_k}}{T_{ACK-R_k}}\right)E_{ACK-R_k,tx} + \left(\frac{\alpha\,\tau\,\pi_{ACK-R_k-A}}{T_{ACK-R_k-A}}\right)E_{ACK-R_k-A,rx}\right] \quad (11)$$

TABLE II: Simulation Parameters

Parameter	Value	Parameter	Value
Operating Frequency	57-64 GHz	P	2200 bytes
Bandwidth	2.16 GHz	t_{sleep}	1 ms
Antenna Height	0.17 m	V	1.8 V
Transmit Power	10 dBm	I_{tx}	661 mA
Realized Antenna Gain	17 dB	I_{rx}	533 mA
Noise Figure	10 dB	I_{idle}	465 mA
Receiver Sensitivity	-49 dBm	I_{sleep}	33 mA

as can be seen from Fig. 2a. In Fig. 2b, the average power consumption grows linearly with R_b when $R_b < R_d$. This arises from the fact that as R_b grows, there is a decrease in the duration for which the geophones remain idle while waiting on packets to get buffered. For the case when $R_b > R_d$, the power consumption tends to conform to a constant value since packets are always being relayed at any given point of time. This is represented by the analysis technique in (9) as well. In all cases, albeit a finite margin of error between analysis and simulation, the overall trend is captured well by the proposed analysis technique.

In Fig. 3, the PSGR scheme is evaluated for $R_b/R_d = 0.5$ as a function of β (integer factors of α) and t_{hold}. In Fig. 3a-3c, the latency grows linearly with β, and the gradient is steeper for larger values of N. For a larger value of β, the number of concurrent transmissions across the geophone chain is reduced, resulting in a larger latency. As t_{hold} increases in value, an increase in latency is observed for the simple reason that an additional delay is introduced at every geophone before performing a transmission. However, the same reasoning leads to enhanced power conservation as seen in Fig. 3d-3f. An increase in latency suggests longer periods of operation during which no transfer of data occurs, during which power is conserved via the repeated sleep/wake-up iterations at intervals of t_{sleep}. However, an abrupt increase in power consumption is witnessed for $\beta \in [2, 20]$ as compared to the case when $\beta = 1$. This arises from the fact that the energy cost associated with the transmission of blocks of β packets outweighs the energy savings obtained while in sleep mode. For much larger values of β however, the number of such blocks is reduced and a decreasing trend for the power consumption is observed.

It can be seen that the trade-off between latency and power consumption is more significant with larger values of N and α. In order to quantify this trade-off, define F to be the amount of power conserved per unit latency. Under the PSGR

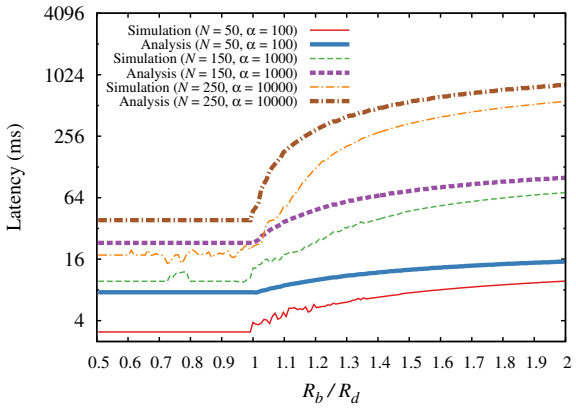

(a) End-to-end latency.

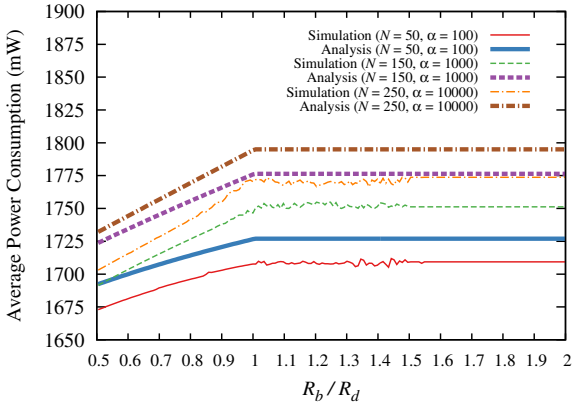

(b) Average power consumption per geophone.

Fig. 2: Analysis vs Simulation

scheme, power conservation can be achieved by altering values for either β or t_{hold}. Let us first consider the impact of varying β for a fixed value of t_{hold}. Comparing between $\beta = 1$ and $\beta = \alpha$ for $t_{hold} = 0$ ms, $F = 1759.35$ mW/s when $N = 50, \alpha = 100$ and $F = 3.75$ mW/s when $N = 250, \alpha = 10000$. This shows that a large value for $\beta = \alpha$ can conserve power very effectively when N and α are small, however, it can be detrimental to the power-saving performance for larger values of N and α. Let us now consider the impact of varying t_{hold} for a fixed value of β. Comparing between $t_{hold} = 0$ ms and $t_{hold} = 25$ ms for $\beta = 1$, $F = 733.09$ mW/s when $N = 50, \alpha = 100$ and $F = 132.23$ mW/s when $N = 250, \alpha = 10000$. Although the

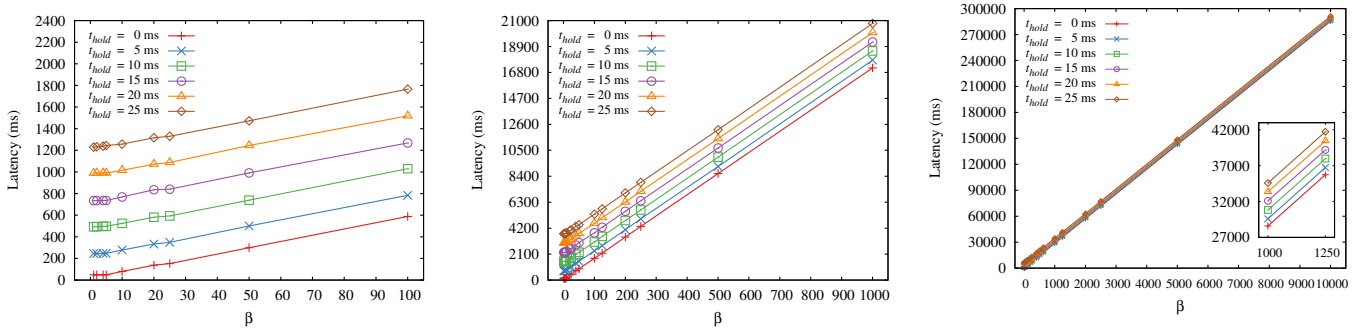

(a) Latency for the case when $N = 50$, $\alpha = 100$.

(b) Latency for the case when $N = 150$, $\alpha = 1000$.

(c) Latency for the case when $N = 250$, $\alpha = 10000$.

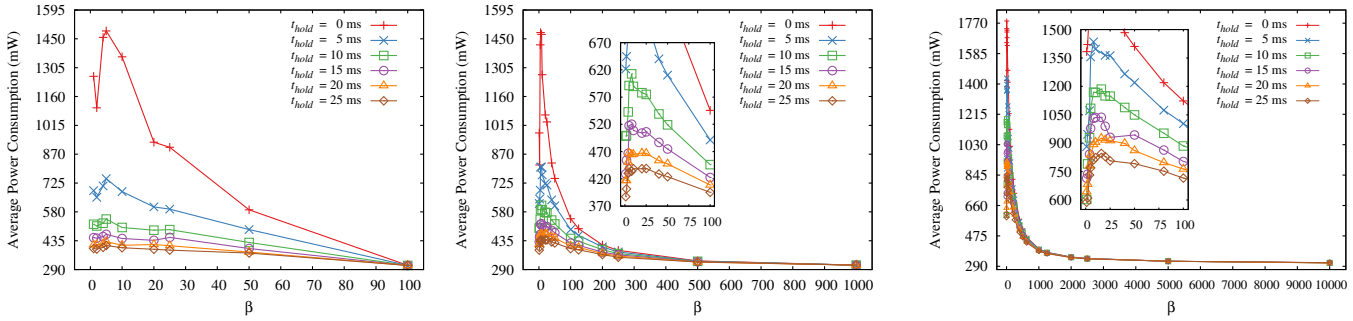

(d) Average power consumption per geophone for the case when $N = 50$, $\alpha = 100$.

(e) Average power consumption per geophone for the case when $N = 150$, $\alpha = 1000$.

(f) Average power consumption per geophone for the case when $N = 250$, $\alpha = 10000$.

Fig. 3: Performance Evaluation of the PSGR scheme

power-saving performance obtained from using higher values of t_{hold} is not as effective as in the case with β for smaller values of N and α, the impact of t_{hold} is not as detrimental as that of β for larger values of N and α. Overall, to obtain effective power-saving at the cost of a minimal increase in latency, a large value for β can be employed when N and α are small, while a large value for t_{hold} can be employed when N and α are large.

V. Conclusion

A multi-channel dual-radio IEEE 802.11ad mesh network is described for use in seismic acquisition and analyzed in terms of the latency and power consumption. The analysis shows that the overall performance is strongly affected by the ratio of the buffering rate to the data transfer rate. An energy-efficient PSGR scheme is also discussed with the objective of conserving power at the cost of an increased latency. While the power conservation performance is remarkable for a smaller number of geophones and data packets, the energy savings come at a significantly greater cost in terms of latency in the case of a larger number of geophones and data packets.

References

[1] C. Bagaini, T. Bunting, A. El-Emam, A. Laake, and C. Strobbia, "Land Seismic Techniques for High-Quality Data," *Oilfield Review*, vol. 22, no. 2, 2010.

[2] D. Crice, "Seismic Surveys Without Cables," *GEO ExPro*, vol. 8, no. 4, pp. 42–46, 2011.

[3] S. Savazzi, U. Spagnolini, L. Goratti, D. Molteni, M. Latva-aho, and M. Nicoli, "Ultra-Wide Band Sensor Networks in Oil and Gas Explorations," *IEEE Communications Magazine*, vol. 51, no. 4, pp. 150–160, April 2013.

[4] D. Crice, "Systems and Methods for Seismic Data Acquisition," *U.S. Patent 9,291,732*, March 2016.

[5] V. A. Reddy, G. L. Stüber, and S. Al-Dharrab, "Energy Efficient Network Architecture for Seismic Data Acquisition via Wireless Geophones," in *IEEE International Conference on Communications (ICC)*, Kansas City, USA, May 2018, pp. 1–5.

[6] V. A. Reddy, G. L. Stuber, S. Al-Dharrab, W. Mesbah, and A. H. Muqaibel, "A Wireless Geophone Network Architecture using IEEE 802.11af with Power Saving Schemes," *IEEE Transactions on Wireless Communications*, pp. 1–16, 2019.

[7] V. A. Reddy, G. L. Stüber, and S. I. Al-Dharrab, "High-Speed Seismic Data Acquisition Over mm-Wave Channels," in *2018 IEEE 88th Vehicular Technology Conference (VTC-Fall)*, Aug 2018, pp. 1–5.

[8] V. A. Reddy, G. L. Stüber, S. Al-Dharrab, W. Mesbah, and A. H. Muqaibel, "Wireless Backhaul Strategies for Real-Time High-Density Seismic Acquisition," in *2020 IEEE Wireless Communications and Networking Conference (WCNC)*, April 2020, pp. 1–5.

[9] F. Tong, L. Zheng, M. Ahmadi, M. Ni, and J. Pan, "Modeling and analyzing duty-cycling pipelined-scheduling mac for linear sensor networks," *IEEE Transactions on Vehicular Technology*, vol. 65, no. 4, pp. 2608–2620, April 2016.

[10] S. Liu, K. Fan, and P. Sinha, "Dynamic Sleep Scheduling using Online Experimentation for Wireless Sensor Networks," in *Proceedings of the Third International Workshop on Measurement, Modeling and Performance Analysis of Wireless Sensor Networks*, July 2005.

[11] I. Villordo-Jimenez, N. Torres-Cruz, M. M. Carvalho, R. Menchaca-Mendez, M. E. Rivero-Angeles, and R. Menchaca-Mendez, "A selective-awakening MAC protocol for energy-efficient data forwarding in linear sensor networks," *Wireless Communications and Mobile Computing*, vol. 2018, pp. 1–18, March 2018.

[12] "IEEE 802.11ad, Amendment 3: Enhancements for Very High Throughput in the 60 GHz Band," pp. 1–628, Dec 2012.

[13] S. Ross, *Introduction to Probability Models (Eleventh Edition)*. Academic Press, 2014.

[14] D. Halperin, B. Greenstein, A. Sheth, and D. Wetherall, "Demystifying 802.11n Power Consumption," in *Proceedings of the 2010 International Conference on Power Aware Computing and Systems*, ser. HotPower'10. Berkeley, CA, USA: USENIX Association, 2010.